Cell

Myelin Gene Regulatory Factor Is a Critical Transcriptional Regulator Required for CNS Myelination

Ben Emery,[1,*] Dritan Agalliu,[1] John D. Cahoy,[1] Trent A. Watkins,[1] Jason C. Dugas,[1] Sara B. Mulinyawe,[1] Adilijan Ibrahim,[1] Keith L. Ligon,[2] David H. Rowitch,[3] and Ben A. Barres[1]

[1]Department of Neurobiology, Stanford University School of Medicine, Stanford, CA 94305-5125, USA

[2]Department of Pediatric Oncology, Dana-Farber Cancer Institute, Harvard Medical School, Boston, MA 02115, USA

[3]Department of Pediatrics, Howard Hughes Medical Institute and Institute for Regeneration Medicine, University of California, San Francisco, San Francisco, CA 94143-0734, USA

*Correspondence: bemery@stanford.edu

DOI 10.1016/j.cell.2009.04.031

SUMMARY

The transcriptional control of CNS myelin gene expression is poorly understood. Here we identify gene model 98, which we have named myelin gene regulatory factor (MRF), as a transcriptional regulator required for CNS myelination. Within the CNS, MRF is specifically expressed by postmitotic oligodendrocytes. MRF is a nuclear protein containing an evolutionarily conserved DNA binding domain homologous to a yeast transcription factor. Knockdown of MRF in oligodendrocytes by RNA interference prevents expression of most CNS myelin genes; conversely, overexpression of MRF within cultured oligodendrocyte progenitors or the chick spinal cord promotes expression of myelin genes. In mice lacking MRF within the oligodendrocyte lineage, premyelinating oligodendrocytes are generated but display severe deficits in myelin gene expression and fail to myelinate. These mice display severe neurological abnormalities and die because of seizures during the third postnatal week. These findings establish MRF as a critical transcriptional regulator essential for oligodendrocyte maturation and CNS myelination.

INTRODUCTION

Myelination in vertebrates has evolved to insulate axons and promote rapid propagation of action potentials. Within the CNS, this function is carried out by oligodendrocytes (OLs). Developmentally, committed OL progenitor cells (OPCs) arise from stereotyped germinal regions of the CNS, proliferate, and migrate throughout the CNS before differentiating into postmitotic premyelinating OLs. These premyelinating OLs subsequently either upregulate myelin genes and ensheath adjacent axons or undergo apoptosis. Several transcription factors are required for the specification of OPCs or their subsequent differentiation into postmitotic OLs, such as Nkx2.2, Sox10, and the bHLH proteins Olig1/2. (Fu et al., 2002; Kuhlbrodt et al., 1998; Lu et al., 2000; Qi et al., 2001; Stolt et al., 2002; Zhou et al., 2001). Among these, Olig2 is the only gene necessary for the OL lineage specification, with *Olig2*$^{-/-}$ mice showing a loss of PDGFRα-positive OPCs within most of the CNS (Lu et al., 2002; Zhou and Anderson, 2002). In contrast, mutants for Olig1, Sox10, and Nkx2.2 have only mild defects in OPC generation, but show impaired oligodendrocyte differentiation and myelin gene expression (Qi et al., 2001; Stolt et al., 2002; Xin et al., 2005). More recently Yin Yang1 (YY1) has also been demonstrated to play an important role in oligodendrocyte differentiation (He et al., 2007).

Few transcription factors function specifically at the postmitotic stage of the OL lineage, and those that do (e.g., Nkx6.2) (Southwood et al., 2004), do not appear to be necessary for most aspects of myelination. It is thus unclear whether the known oligodendrocyte lineage transcription factors play a dual role in oligodendrocyte differentiation and myelination, or instead are required only for oligodendrocyte differentiation, with other yet-to-be-identified transcription factors playing essential roles in inducing myelin gene expression and the transition to a myelinating OL. This situation contrasts with that of PNS myelination, where the transcription factor Krox-20 (expressed in myelinating Schwann cells) is both sufficient and necessary to induce myelin gene expression and myelination in these cells (Nagarajan et al., 2001; Topilko et al., 1994). As such, the nature of transcriptional control of the final stages of OL maturation including myelin gene expression remains unclear.

In a recent study, we determined the transcriptomes of acutely isolated astrocytes, neurons, and OLs from the postnatal mouse forebrain (Cahoy et al., 2008). We identified gene model 98 as a gene expressed within the CNS only by postmitotic OLs. Here, we demonstrate that gene model 98, which we have named myelin gene regulatory factor (MRF), is necessary for the generation of mature myelin-gene-expressing OLs within the CNS. RNAi-mediated knockdown of MRF in cultured OPCs does not affect their exit from the cell cycle and downregulation of OPC markers, but markedly reduces the expression of the majority of myelin genes. Conversely, overexpression of MRF

within cultured OPCs is sufficient to induce myelin gene expression, and it can promote myelin gene expression in the developing chick spinal cord. Moreover, we show that mice in which MRF function is disrupted within the OL lineage show severe dysmyelination. Although premyelinating OLs are generated in these mice, these premyelinating OLs fail to upregulate myelin gene expression and ensheath axons, and instead undergo apoptosis. These results establish MRF as a transcriptional regulator vital for the generation of myelinating OLs, with an analogous role in the CNS to that of Krox-20 in the PNS.

RESULTS

GM98/MRF Is an OL-Specific Nuclear Protein within the CNS

We used an immunopanning/FACS cell purification approach combined with gene profiling in order to identify cell-type-specific genes within the mouse CNS (Cahoy et al., 2008). Among the genes displaying OL-specific expression was gene model 98. The Affymetrix probe set for this gene was absent in samples derived from astrocytes and neurons, present at very low levels in OPCs, but upregulated in newly differentiated (GC^+, MOG^-) and mature (MOG^+) OLs (Figure 1A). Northern blotting confirmed that MRF was present in brain and OL samples as a ~5.5 kb transcript, consistent with database predictions (Figure 1B). In situ hybridization showed that MRF displayed the same distribution as the established OL marker PLP, with expression largely confined to white matter tracts within the CNS (Figure 1C). The expression of MRF by myelinating cells was CNS specific, with no expression detected in the PNS (Figure S1 available online).

Sequencing of cDNA derived from cultured mouse OLs predicted a protein of 1139 amino acids, with an overall identity of 88.6% to the human gene C11Orf9 (Figure S2). The protein contained a predicted DNA binding region homologous to the yeast transcription factor Ndt80 (Montano et al., 2002); within this region, MRF and C11Orf9 shared 100% sequence identity (Figure 1D). C11Orf9 has been postulated to be a transmembrane protein based on the presence of hydrophobic regions in the C-terminal region (Stohr et al., 2000). In order to assess the subcellular localization of MRF, we expressed a myc-tagged version of the protein and probed with anti-myc; the fusion protein had a nuclear localization when expressed in both HEK cells (Figure 1E) and cultured OLs (data not shown). These data provide evidence that MRF is a nuclear protein displaying OL-specific expression within the CNS.

In order to assess whether MRF displayed a developmental expression profile consistent with a role in myelination, we performed in situ hybridization on brain sections of mice at postnatal days 3 to 21. At P3, the expression of MRF was restricted to cells in the hindbrain and cerebellum, subsequently spreading rostrally throughout the white matter tracks over the first 2 weeks postnatal, mirroring the expression of PLP (Figure 1F). Dual fluorescent in situ hybridization for MRF and PLP revealed that within the cerebellum at early ages (P3 and P7), many MRF^+ cells were either PLP^- or only weakly PLP^+ (arrowheads, Figure 1G). At later ages (P14 and P21), however, the two genes showed near 100% colocalization. This suggests that the expression of MRF may slightly precede that of myelin genes such as PLP within differentiating oligodendrocytes. Similarly, northern blots revealed that MRF transcript was absent in the P1 brain but steadily increased from P3 to P14, peaking in expression before PLP transcript (Figure S1). Within the embryonic spinal cord, a few MRF^+ cells were detected by E17, in a pattern similar to PLP and MBP (Figure S1). These results confirmed that MRF has an expression pattern consistent with a potential role in myelination.

Knockdown of MRF in Cultured OLs Blocks Myelin Gene Expression

To establish whether MRF may have a role in OL differentiation or myelin gene expression, we transfected cultured mouse OPCs with control nontargeting siRNA pool (siCont) or pooled siRNAs against MRF (siMRF). Knockdown of MRF was confirmed by northern blot and RT-PCR (Figure 2E and data not shown). siMRF-transfected OPCs displayed no obvious deficiencies when cultured in the presence of PDGF, which promotes the growth of progenitor cells (data not shown). When transfected OPCs were instead plated into media lacking PDGF and with T3 to induce their differentiation into OLs (Dugas et al., 2006), the siMRF-transfected cells showed both delayed and reduced levels of MBP expression relative to siCont-transfected cells and failed to express MOG even after 4 days of differentiation, by which time the majority of siCont-transfected cells expressed MOG (Figures 2A–2D). This failure of siMRF-transfected cells to express MBP and MOG was not due to a failure of differentiation per se or a diversion to an astrocyte fate; the siMRF-transfected cells still downregulated the OPC marker NG2, did not express the astrocyte marker GFAP, were positive for the OL marker GalC, and took on the multipolar morphology characteristic of OLs, albeit with far less extensive membrane sheets than siCont-transfected cells (Figure S3C). This effect was unlikely to be mediated by off-target siRNA effects, because it was observed with 2 of 4 independent nonoverlapping siRNA constructs targeting MRF (Figure S3E). Interestingly, after 2 days of differentiation, the MRF knockdown resulted in an increased apoptosis relative to siCont-transfected cells (Figure S3). Although mouse OLs have a limited viability in culture after differentiation with few cells surviving more than a week, the rate of apoptosis was accelerated in cells transfected with siMRF compared to siCont. Furthermore, siMRF-transfected cells showed decreased expression of other myelin genes CNP and PLP (Figure 2D).

To further characterize the changes in gene expression resulting from inhibition of MRF expression, we performed GeneChip analysis between OL cultures differentiated for 2 days after transfection with siCont or siMRF and OPC cultures that served as a measure of baseline gene expression prior to differentiation. The GeneChip analysis confirmed that upon differentiation both siCont- and siMRF-transfected cultures completely downregulated OPC markers (e.g., NG2, PDGFRα, and Ki67) (Figure 2F). In addition, siMRF-transfected cultures failed to induce most myelin genes, with the expression of late phase genes such as MAG and MOBP being entirely blocked (the 50 most repressed genes by siMRF are listed in Table S1) relative to the siCont cultures. Most early OL genes such as MBP and PLP were also inhibited, though to a lesser extent, and pan-OL lineage genes

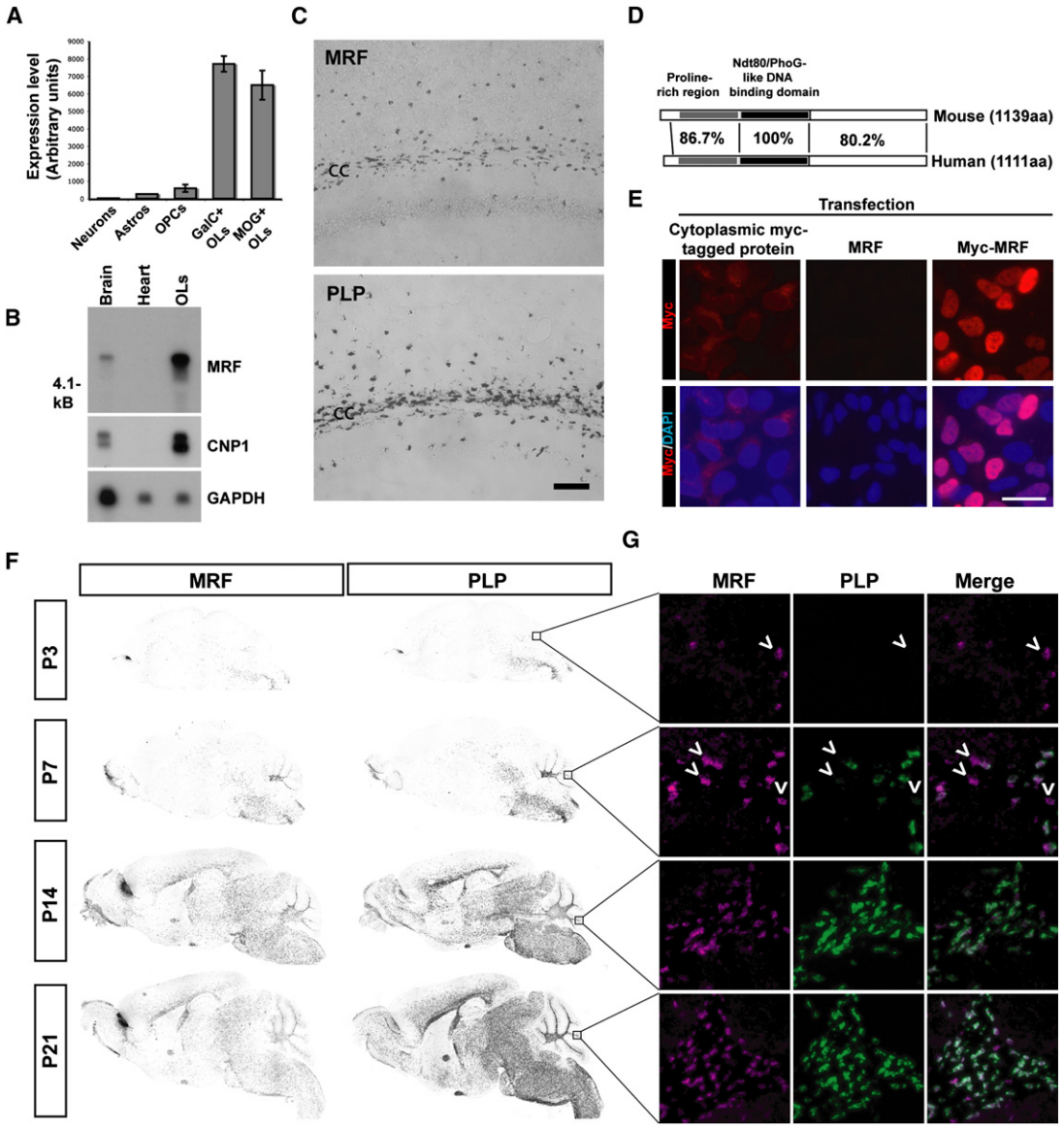

Figure 1. GM98/MRF Is a Nuclear Protein Specifically Expressed within the CNS by Postmitotic OLS

(A) Affymetrix expression levels of GM98/MRF in acutely isolated cells from the mouse CNS (probe set 1439506_at). Expression was considered present by GCOS software for the OPC, GalC$^+$ OL, and MOG$^+$ OL samples.

(B) Northern blot confirmed expression of MRF as a single ~5.5 Kb transcript within P20 brain and cultured OLs, but not heart tissue, similar to OL marker CNP. GAPDH controls for mRNA loading.

(C) In situ hybridization for PLP and MRF expression within the lateral corpus callosum (cc) and scattered cells in the overlying cortex. Scale bar represents 100 μm.

(D) Schematic of the protein domains of GM98/MRF and the human ortholog C11Orf9, showing percent identity in each region.

(E) Subcellular localization of myc-tagged MRF within HEK cells. Staining of Myc-MRF-transfected HEK cells with anti-myc indicates a predominantly nuclear localization of the protein, with colocalization with the nuclear counterstain DAPI in transfected cells. Non-myc-tagged MRF and a myc-tagged protein displaying a cytoplasmic localization provide a negative control for the staining and a comparison, respectively. Scale bar represents 50 μm.

(F) In situ hybridization for MRF and PLP in P3-21 sagittal brain sections showing their developmental expression profile.

(G) Double fluorescent in situ hybridization for MRF and PLP in the white matter of the developing cerebellum (P3–P21); arrowheads indicate MRF$^+$/PLP$^-$ cells.

such as Sox10, Olig1, and Olig2 were unaffected by the MRF knockdown (Figure 2G). Interestingly, when the genes repressed 4-fold or more by the MRF knockdown were compared to the genes induced during OL differentiation (between OPC and siCont samples), the majority of genes dependent on MRF expression were genes usually induced specifically in OLs during their differentiation (104 of 128 probe sets). MRF-regulated genes represented only a subset of genes that are normally induced during OL differentiation (104 of 793 probe sets), whereas the expression of other OL-specific genes such as

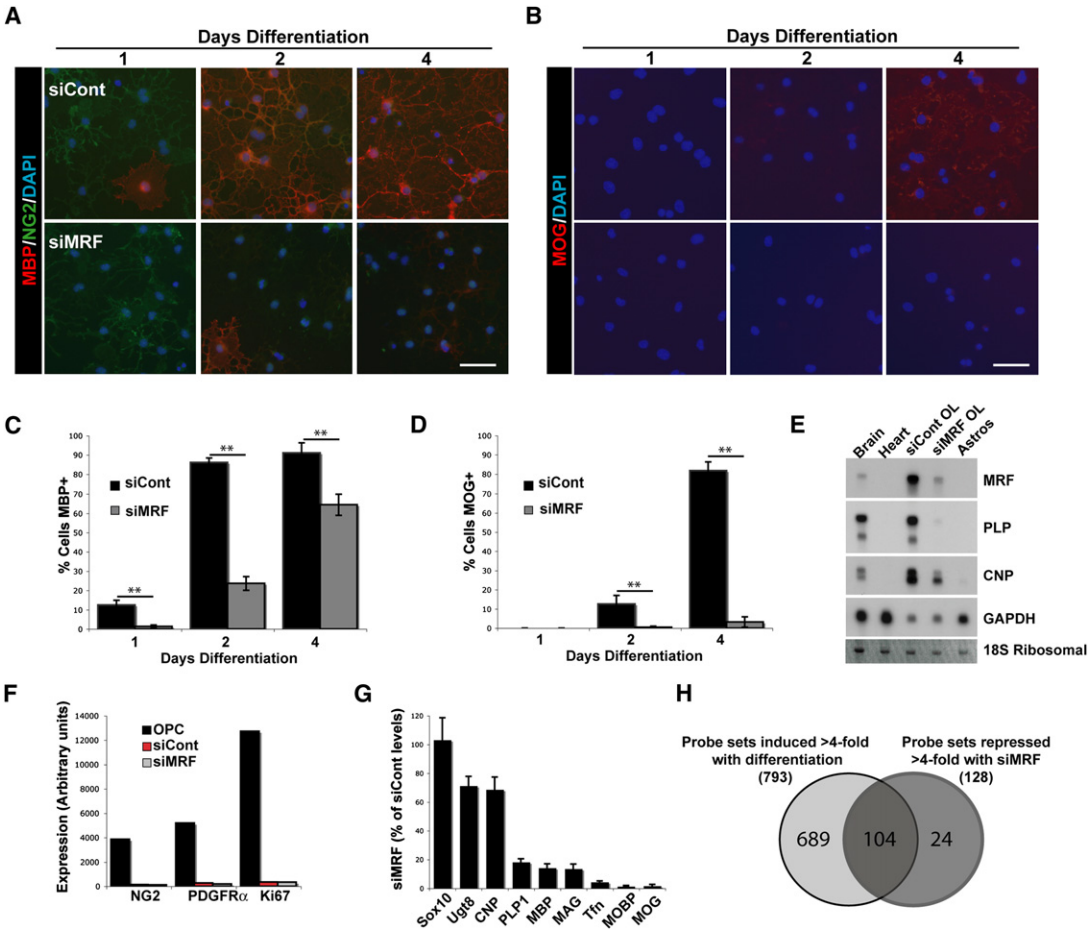

Figure 2. Knockdown of MRF in OLs Blocks Myelin Gene Expression

(A and B) Representative images of OL cultures transfected with siCont or siMRF and differentiated for 1, 2, and 4 days stained with NG2 and MBP (A) or MOG (B). Scale bars represent 50 μm.

(C and D) Quantification of the proportion of siCont- and siMRF-transfected OLs expressing MBP (C) and MOG (D) at 1, 2, and 4 days differentiation. **$p < 0.01$.

(E) Northern blot analysis of gene expression in siCont- and siMRF-transfected OL cultures at 2 days differentiation. RNA from brain, heart, and cultured astrocyte samples are provided for positive and negative controls, respectively.

(F and G) Results of GeneChip analysis of gene expression in OPCs and OLs transfected with siCont or siMRF as OPCs then cultured for 2 days in differentiating conditions.

(F) Downregulation of selected OPC markers NG2, PDGFRα, and Ki67 during differentiation is not affected by MRF knockdown.

(G) Expression of OL pan-OL lineage marker Sox10, early-OL markers (Ugt8, CNP, PLP, and MBP), and late-OL markers (MAG, transferrin/Tfn, MOBP, and MOG) in cells transfected with siMRF expressed as a mean percentage of siCont-transfected OL values ± SEM. Results are averages of three independent experiments.

(H) Venn diagram showing overlap of genes induced >4-fold with differentiation and those repressed >4-fold by transfection with siMRF.

Cldn11/OSP or cell cycle regulators was largely unaffected (Figure 2H). These findings indicate that MRF is required for the induction of most CNS myelin genes and many, albeit not all, OL-specific genes involved in oligodendrocyte maturation.

Forced MRF Expression Induces Myelin Gene Expression In Vitro and In Vivo

We next asked whether the expression of MRF was sufficient to induce the expression of myelin genes. We transfected mouse OPCs with a GFP expression plasmid together with either a plasmid encoding MRF or an empty control vector and plated them in media containing PDGF to maintain their growth as OPCs. Cells transfected with the control vector (identified by GFP expression) remained $NG2^+$, MBP/MOG^- OPCs (Figure 3A). In contrast, MRF-transfected cells downregulated NG2, upregulated MBP and MOG, and acquired a flattened morphology (Figure S4). This effect was evident by 2 days posttransfection and was more pronounced at 5 days posttransfection, by which time approximately 80% of the MRF-transfected cells expressed MBP and MOG (Figures 3B and 3C). In this assay, the induction of MBP and MOG expression by MRF was considerably more pronounced than that seen with Sox10, a gene that promotes MBP expression and OL differentiation (Li et al., 2007; Stolt et al., 2002).

To assess whether forced expression of MRF could also induce myelin gene expression in vivo, we electroporated HH

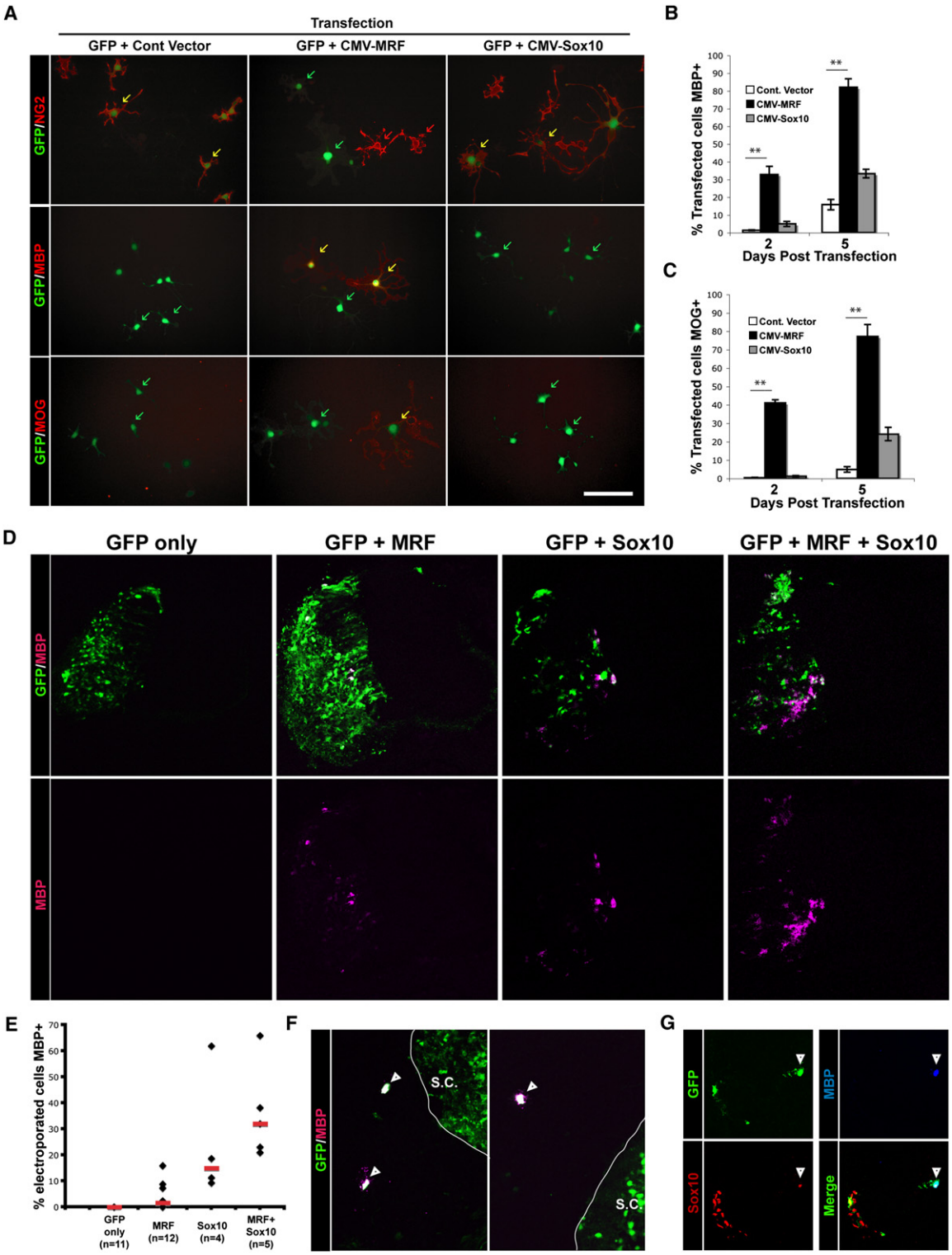

Figure 3. Forced MRF Expression Induces Myelin Gene Expression In Vitro and In Vivo

(A) Representative images of mouse OPCs cotransfected with eGFP and control (empty) vector, or vectors encoding MRF or Sox10 and then cultured for 2 days posttransfection in proliferative conditions. Cells are stained for the OPC marker NG2 or OL markers MBP and MOG. Scale bar represents 50 μm.

(B and C) Quantification of the proportion of transfected cells in each condition expressing MBP (B) and MOG (C) at 2 and 5 days posttransfection. **$p < 0.01$, unpaired t test. Values are means ± SEM.

stage 12–14 chick spinal cords with either a GFP plasmid or GFP and MRF plasmids and analyzed the embryos 4 days later at HH stage 27–28, prior to the normal differentiation of OLs in the chick spinal cord (Zhou et al., 2001). Immunostaining revealed scattered MBP$^+$ cells on the electroporated side of the spinal cord; such cells were never observed on the non-electroporated side or in GFP-only electroporated controls (Figures 3D and 3E). Misexpression of MRF in the chick spinal cord induced MBP expression only in a small subset of GFP$^+$ cells (ranging from 0% to 15.9% of GFP$^+$ cells in various animals, median = 1.6%), a phenotype that was different to that seen in cultured mouse OPC, where forced MRF expression induced myelin gene expression in a high percentage of cells. Interestingly, a high percentage (31.7%) of neural-crest-derived cells that were electroporated with MRF (GFP$^+$ and Sox10$^+$ cells outside the spinal cord) ceased to migrate shortly after leaving the dorsal spinal cord and upregulated MBP expression (Figures 3F and 3G). MBP expression in GFP$^+$ neural crest cells was never observed in GFP-only-electroporated embryos. These results suggested that these cells expressed transcription factors that in combination with MRF induced MBP expression.

To investigate this possibility, we electroporated Sox10, a neural crest marker, or Sox10 and MRF in chick spinal cord and assayed MBP expression after 4 days. Sox10 electroporation induced a larger number of MBP$^+$ cells compared to MRF electroporation (ranging from 9.3% to 61.9% of GFP$^+$ cells in different animals, median = 14.9%). However, coelectroporation of MRF and Sox10 increased the number of MBP$^+$ cells compared to Sox10 alone (ranging from 20.9% to 65.8% of GFP$^+$ cells in different animals, median = 32.0%), but this difference was not statistically significant because of a high variability in MBP induction between animals. These results indicate that MRF is able to induce myelin gene expression in vivo as well as in cultured OPC cultures, but may cooperate with other transcription factors (e.g., Sox10) to promote myelination in vivo.

MRF Expression Is Necessary for CNS Myelination

To assess the role of MRF in mammalian CNS myelination, we generated an *MRF* allele where exon 8 was flanked by loxP sites (see Figure S5A for a description of the targeting vector). Exon 8 codes part of the predicted DNA binding region of MRF; as such, Cre-mediated excision of exon 8 was predicted to result in a truncated protein lacking the DNA binding region and subsequent C-terminal region of the protein resulting from a frame shift (Figure S5B). Initial experiments overexpressing this predicted post-excision protein in OPCs confirmed that it had no ability to induce myelin gene expression, unlike the full-length protein (data not shown). We crossed the *MRF* loxP-flanked exon 8 ($MRF^{fl/fl}$) mice with an *Olig2-Cre* knockin mouse line (Schuller et al., 2008) to effect recombination in glia including the OL lineage from an early developmental stage. We confirmed successful deletion of *MRF* exon 8 by RT-PCR of cDNA samples from spinal cords and cultured OLs from *MRF* CKOs (Figure S9).

MRF conditional knockout (CKO) mice ($MRF^{fl/fl}$; $Olig2^{wt/cre}$) were born at Mendelian frequencies and were not overtly distinguishable from control littermates ($MRF^{wt/fl}$; $Olig2^{wt/cre}$ and $MRF^{fl/fl}$; $Olig2^{wt/wt}$) for the first 10 days of life. From P11, however, CKOs developed severe tremors and ataxia (Movie S1), subsequently also developing seizures and dying during the third postnatal week (Figure 4). Immunohistochemical analysis of the brains of CKO mice at P13 (Figure 4A) indicated that NeuN and GFAP staining appeared normal and that the gross CNS cytoarchitecture was not affected. In contrast, there was a severe loss of staining for MBP within the brain, with only occasional MBP$^+$ oligodendrocytes seen within white matter tracts, compared to near-ubiquitous MBP staining in the white matter tracts of control mice. CKO spinal cords also showed a severe loss of MBP immunostaining (Figure 4B), although the spinal roots (myelinated by Schwann cells) still stained intensely for MBP. As with the brains, NeuN and GFAP staining were unaffected by the conditional deletion of MRF. Similarly, ChAT immunostaining indicated that the motor neuron population was intact in CKOs, indicating that disruption of the *MRF* gene does not directly affect motor neurons (MNs are derived from Olig2$^+$ progenitors and should undergo Olig2-Cre-mediated recombination). At higher magnification, some faintly MBP$^+$ cells with the morphology of premyelinating OLs could be seen in the brains and spinal cords (Figures S6 and S7), suggesting that the early stages of OL differentiation did occur in the absence of MRF expression.

We confirmed loss of myelin protein expression in the CKO by western blot of P13 spinal cord lysates, which demonstrated substantially less MBP and CNP expression and a complete loss of MOG expression in CKOs relative to control genotypes (Figure 4C). Astrocyte and neuron proteins (GFAP and neurofilament, respectively) were not affected in the CKO. To confirm a loss of myelin proteins at other stages of development, we harvested brains from CKOs and controls from P7 (at which stage myelination in the brain is just beginning) to P17 (the latest the CKOs could be reliably studied, because of their death). The brains of control mice showed a substantial upregulation of the proteins MBP, CNP, and MOG during this time; at all time points, MBP and MOG were near undetectable in the CKOs (Figure 4D), although some MBP expression was seen at very long exposures (data not shown).

Fluoromyelin staining within CNS white matter tracts of CKOs revealed a complete loss of myelination in CKO animals (Figure 4E). In contrast, peripheral nerves were equivalently myelinated in both CKOs and controls as expected, as shown by the fact that Schwann cells express neither MRF nor Olig2. We confirmed the loss of myelination by electron microscopy in

(D) Representative spinal cord sections of chicken embryos electroporated with expression constructs for MRF, Sox10, or both genes at E3 (stage 12) along with a GFP construct and allowed to develop until E7. Sections are stained with anti-MBP, with GFP shown to identify electroporated cells.

(E) Quantification of the proportion of electroporated cells expressing MBP for each condition; shown are values for individual animals and median values for each condition (red bars).

(F and G) Examples of MRF-electroporated neural crest cells ectopically expressing MBP (F); (G) shows triple labeling for GFP, MBP, and Sox10. The arrowhead indicates a triple-labeled cell; a GFP/Sox10$^+$, MBP$^-$ cell can be seen to the left of the image.

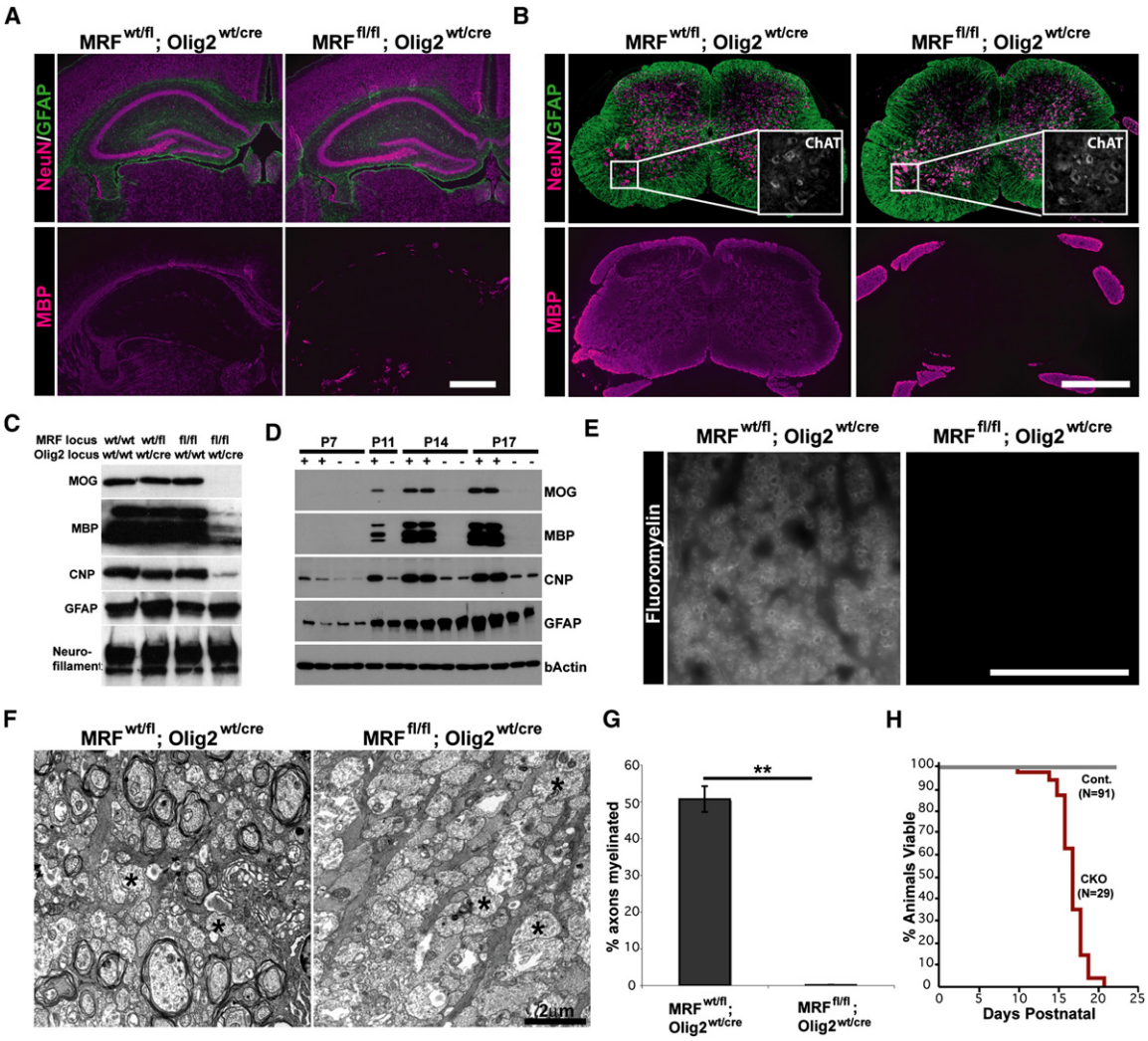

Figure 4. *MRF* CKOs Display CNS Dysmyelination

(A and B) Representative images of the hippocampus, corpus callosum, and overlying cortex (A) and spinal cord (B) of control ($MRF^{wt/fl}$; $Olig2^{wt/cre}$) and *MRF* CKO ($MRF^{fl/fl}$; $Olig2^{wt/cre}$) mice stained with MBP, NeuN, and GFAP at P13. ChAT staining of spinal cord motor neurons is shown in the inserts of (B).

(C) Western blot analysis of CNP, MBP, MOG, GFAP, and Neurofillament expression in the spinal cords of *MRF* control and CKO mice at P13.

(D) Developmental time-course of myelin gene expression in the brains of *MRF* control (+) and CKO (−) mice with CKOs showing severe deficit in MBP and MOG expression.

(E) Representative images of Fluoromyelin staining of the spinal cord lateral column white matter in a control ($MRF^{wt/fl}$; $Olig2^{wt/cre}$) and CKO ($MRF^{fl/fl}$; $Olig2^{wt/cre}$) mouse at P13.

(F) Representative electron micrograph images of control and CKO optic nerves at P13. Control nerves show a significant amount of myelination in progress. In contrast, essentially all axons in the CKOs lack myelin ensheathment (examples denoted by asterisk).

(G) Proportions of axons myelinated for control and CKOs are quantified.

(H) The lifespan of *MRF* CKOs is essentially limited to the third postnatal week.

Scale bars represent 1 mm in (A) and (B), 50 μm in (E), and 2 μm in (F). **$p < 0.01$.

the optic nerves of CKOs; whereas control optic nerves were actively myelinating by P13 with 50.7% ± 3.5% of axons having two or more myelin wraps, virtually no myelination was observed in the optic nerves of CKO littermates, and only 0.07 ± 0.07% of axons were ensheathed ($p < 0.001$, Figures 4F and 4G). Importantly, we saw an equivalent phenotype (tremors, seizures, loss of myelin gene expression/myelination and death in the third postnatal week) when we crossed MRF^{fl} mice with mice expressing Cre recombinase behind the *CNP* promoter (Lappe-Siefke et al., 2003), confirming that the CKO phenotype was not dependent on the *Olig2* heterozygous background caused by insertion of the Cre gene (Figure S6).

OLs Differentiate in *MRF* CKO Mice but then Undergo Apoptosis

To determine which populations of the OL lineage were affected by the loss of MRF, we assessed the densities of OPCs and OLs in P13 CKO and control littermate optic nerve sections

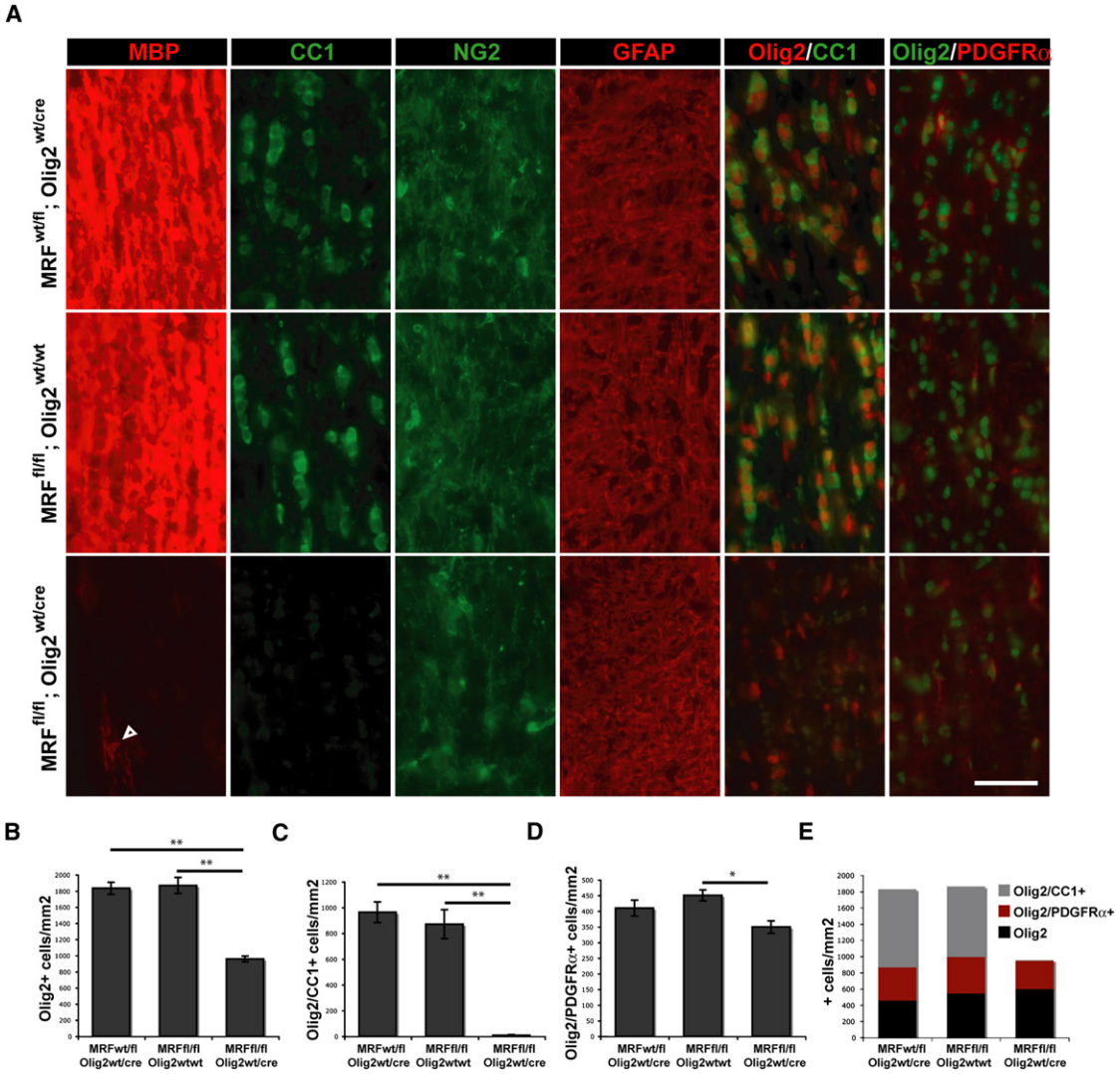

Figure 5. *MRF* CKOs Display a Loss of Mature OLs

(A) Immunostaining for MBP, CC1, NG2, GFAP, and Olig2 costained with CC1 and PDGFRα within the optic nerves of control ($MRF^{wt/fl}$; $Olig2^{wt/cre}$ and $MRF^{fl/fl}$; $Olig2^{wt/wt}$) and *MRF* CKO ($MRF^{fl/fl}$; $Olig2^{wt/cre}$) mice at P13. Scale bar represents 50 μm.

(B) Quantification of the density of Olig2 immunopositive nuclei within the optic nerves.

(C) Quantification of the density of $Olig2^{+}/CC1^{+}$ double-immunopositive OLs within the optic nerves.

(D) Quantification of the density of $Olig2^{+}/PDGFR\alpha^{+}$ double-immunopositive OPCs within the optic nerves. All results are expressed as means ± SEM, n = 4–5 per genotype. *$p < 0.05$, **$p < 0.01$.

(E) Densities of Olig2 immunopositive cells within the optic nerves of each genotype broken down into $Olig2^{+}$ cells also positive for either CC1 (OLs), PDGFRα (OPCs), or neither marker.

(Figure 5A). We found a ~45% reduction in the density of $Olig2^{+}$ nuclei within the optic nerves of CKOs relative to control littermates; this reduction was accounted for by the complete loss of $CC1^{+}$ cells (a marker of postmitotic OLs) in CKO mice (Figures 5B, 5C, and 5E). In contrast, the density of $Olig2^{+}$ and $PDGFR\alpha^{+}$ cells (OPCs) was only modestly reduced (18.7%) in CKOs relative to $MRF^{fl/fl}$; $Olig2^{wt/wt}$ mice (t test $p < 0.05$, but not significantly different from $MRF^{wt/fl}$; $Olig2^{wt/cre}$ controls; Figures 5D and 5E). Therefore, the OPC stage was minimally affected in CKOs, an observation supported also by normal NG2 staining. Similarly, the density of $Olig2^{+}$ cells negative for both CC1 and PDGFRα (presumably Olig2-expressing astrocytes) was similar between genotypes (Figure 4E). Although MBP staining was nearly absent in the CKO optic nerves, a small number of weakly MBP^{+} cells were present, suggesting that at least some postmitotic OLs were generated in the CKO mice. The density of these faintly MBP^{+} cells (35 ± 4 cells/mm^2) was only ~4% of the density of mature OLs in the control mice, and they had the morphology of premyelinating OLs, with thin, nonmyelinating processes aligned with the axons.

To assess whether myelin or mature OLs were present in the CKOs at earlier ages, we examined sagittal sections of the P7

CKO and control brains for MBP, CC1, and PDGFRα expression (Figure S7). The density of OPCs was equivalent in control and CKO mice in both areas studied at P7. Control littermates displayed a caudal to rostral gradient of myelination, with substantial MBP expression in the hindbrain and cerebellum and scattered MBP^+ cells in the more rostral white matter tracts. In contrast, only scattered faintly MBP^+ cells were seen in the CKOs and there was an almost complete absence of MBP or $CC1^+$ cells in the hindbrain ($p < 0.01$). Control mice displayed a mix of premyelinating MBP^+ OLs and myelinating OLs within the corpus callosum at P7 when myelination is proceeding (Figures S7E and S7F). In contrast, only premyelinating MBP^+ but no myelinating OLs were observed in the corpus callosum of CKO mice, indicating that the absence of MRF expression caused a block in the transition from a premyelinating OL to a mature, myelinating OL.

During development, approximately 50% of the postmitotic OLs generated in the CNS undergo apoptosis (Barres et al., 1992; Trapp et al., 1997). The extreme paucity of myelinating OLs seen in CKO mice at P13 combined with the presence of significant numbers of premyelinating OLs at P7 suggested that in the absence of MRF, OLs may undergo apoptosis. We observed that many weak MBP^+ premyelinating OLs in the CKOs displayed the characteristic morphology of apoptotic OLs, with fragmented nuclei and blebbed processes. Staining of optic nerves from P10 CKO and control mice with an antibody against activated caspase-3, a marker of apoptosis, confirmed a significant ~2-fold increase in the density of apoptotic cells in the CKO mice ($p < 0.05$, Figure S8). These data indicate that postmitotic OLs are generated in the *MRF* CKO mice but then undergo apoptosis.

Dysmyelination in *MRF* CKOs Is Cell Autonomous and Not Solely due to Cell Death

It has been proposed that some premyelinating OLs undergo apoptosis because they fail to receive axonal support. If MRF-deficient OLs are unable to upregulate proteins required for interactions with axons, this may explain their apoptosis in vivo. In order to determine whether this is the case for MRF-deficient cells, we cultured highly purified OPCs isolated from P7 control and CKO mice. In the presence of PDGF, both control and CKO OPCs proliferated as NG2 and $Ki67^+$ cells, confirming that MRF is not required for the OPC phase of the OL lineage (Figure 6A). Upon withdrawal of PDGF, both control and CKO cells downregulated Ki67, took on the morphology of OLs, and expressed CNP (Figure 6B). However, CKO cells extended considerably less extensive membrane sheets on the substrate compared to control cells, and expressed low, barely detectable levels of MBP. As in vivo, the MRF-deficient cells showed a significant acceleration of cell death relative to the control genotypes, with 44.2% ± 2.9% of $MRF^{fl/fl}$; $Olig2^{wt/cre}$ cells viable at 4 days differentiation, compared to 64.9% ± 0.5% of $MRF^{fl/fl}$; $Olig2^{wt/wt}$ cells and 61.3% ± 1.4% of $MRF^{wt/fl}$; $Olig2^{wt/cre}$ cells (Figures 6C and 6D, $p < 0.01$). This suggests that the increased apoptosis of CKO OLs in vivo may not solely be due to a loss of axonal support when these cells fail to myelinate, but premyelinating OLs undergo an intrinsic apoptotic program if they cannot induce myelin gene expression and myelinate.

We analyzed RNA from control and CKO spinal cords and OL cultures by RT-PCR and GeneChip microarrays. The expression of many myelin genes such as MAG and MOBP was abolished in both CKO spinal cords and OL cultures, demonstrating a requirement of MRF for the expression of these genes (Figures 6E–6G; Table S1, Figure S7). Because of the substantial loss of OLs in the CKO spinal cords, these samples displayed a loss of essentially all genes specific to postmitotic OLs, whereas cultured CKO cells showed more restricted deficits. The effects of MRF deficiency on OL gene expression in vitro were very similar to those we observed with siMRF knockdown (Figures 6E–6G; Tables S1 and S2), with most myelin genes and many OL maturation genes being strongly downregulated but only moderate effects on several early OL genes such as Ugt8. Interestingly, several genes such as p57/cdkn1c whose expression is normally limited to transient expression by newly formed oligodendrocytes were substantially upregulated in MRF-deficient OLs in vitro, again consistent with the idea that in the absence of MRF, OLs are stalled in the immature, premyelinating stage.

Although the increased apoptotic rate of CKO cells appeared less severe than the deficits in myelin gene expression, it was difficult to ascertain whether these cells undergo apoptosis because of a blockade to transition toward a mature phase, or whether the failure of myelin gene expression was secondary to early apoptosis. To clarify this issue, we infected control and CKO OPCs in vitro with a control adenovirus (Ad-GFP) or a Bcl-2 adenovirus (Ad-Bcl-2) to block apoptosis, induced their differentiation, and assayed survival and myelin protein expression at 2–8 days of differentiation (Figure 7). Infection of cells with Ad-Bcl-2 (Figure 7A) successfully blocked the increased apoptosis of CKO cells relative to control cells, with 74.7% ± 1.6% of control and 75.9% ± 1.9% of CKO cells ($p > 0.05$) remaining viable at 6 days of differentiation, a time at which nearly all of the Ad-GFP-infected cells of both genotypes were dead (15.5% ± 1.3% of control and 15.0% ± 2.4% of CKO cells being viable; Figures 7B and 7C). In spite of the excellent viability of both genotypes when infected with Ad-Cre, the CKO cells still showed a clear deficit in myelin protein expression, whereas the vast majority of control cells were positive for MBP (95.8% ± 1.9%), MAG (96.0% ± 1.7%), and MOG (94.3% ± 2.8%); only 71.5% ± 2.0% of CKO cells were faintly MBP^+, and virtually no CKO cells were positive for MAG (1.2% ± 0.5%) or MOG (0.8% ± 0.3%). The CKO cells also still displayed a less mature morphology than did control cells (Figure 7C) at 6 and 8 days postdifferentiation, a time sufficient to induce the expression of even late-phase myelin genes (Figures 7D–7H; Dugas et al., 2006). Therefore, the apoptosis observed in MRF-deficient OLs is likely to be a secondary effect because of their inability to transition to a mature state.

DISCUSSION

MRF Is a Transcriptional Regulator of CNS Myelin Gene Expression and Plays a Role in the CNS Comparable to that of Krox-20 in the PNS

In this study, we have identified gene model 98/MRF as a transcriptional regulator required for OL maturation and CNS myelination. MRF is not detectably expressed by OPCs, neurons, or

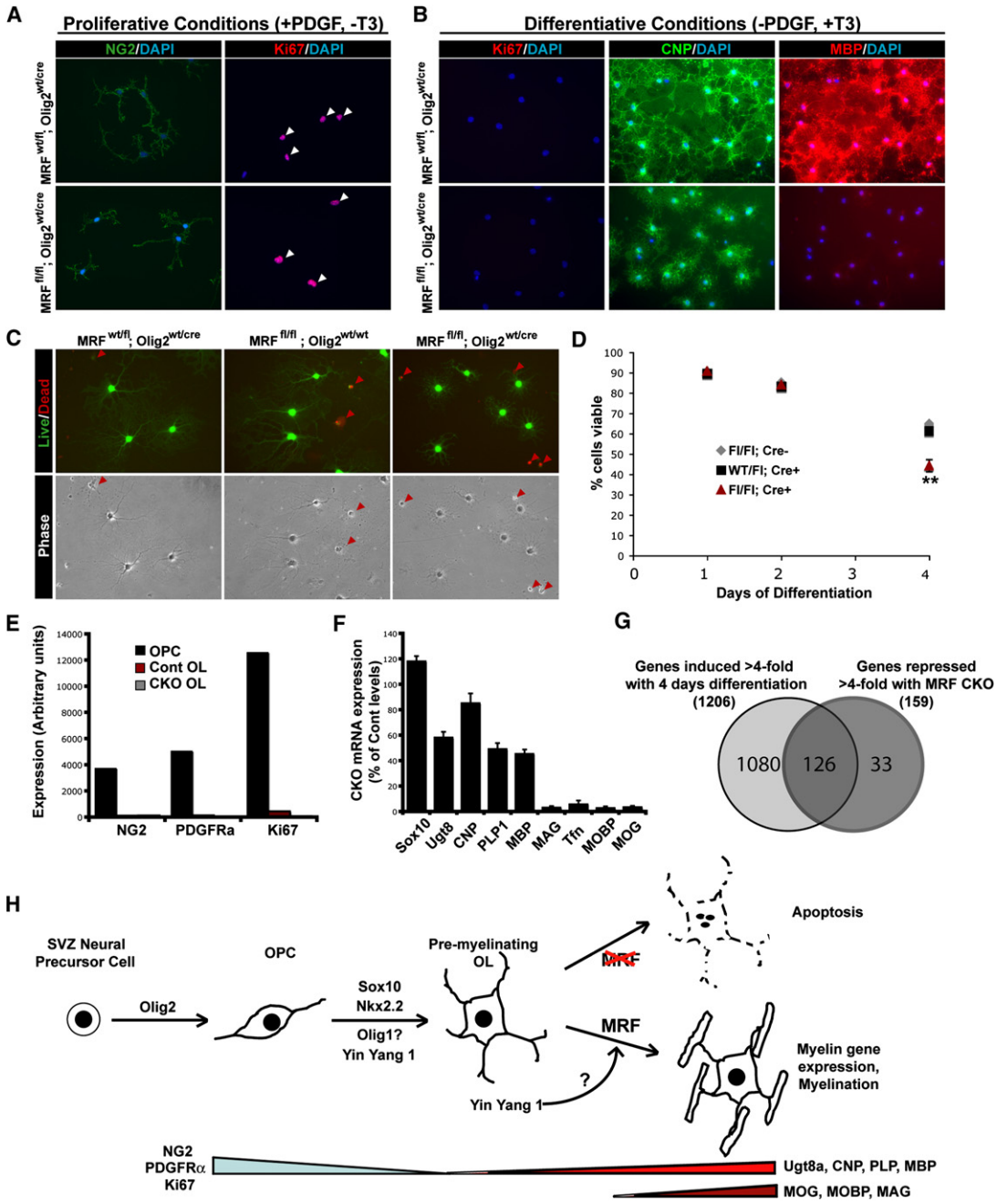

Figure 6. MRF-Deficient OPC/OL Cultures Display Deficiencies in Differentiative, but Not Proliferative, Conditions

(A and B) Immunostaining of control (*MRF$^{wt/fl}$; Olig2$^{wt/cre}$*) and CKO (*MRF$^{fl/fl}$; Olig2$^{wt/cre}$*) cultures for NG2 and Ki67 in proliferative (A) or differentiative (B) conditions. Arrowheads indicate Ki67^{+} nuclei. The same cells stained for CNP and MBP are shown in (B).

(C) Representative images of control and CKO cells stained with calcein AM (green; live cells) and ethidium homodimer (red; dead cells) at 4 days differentiation showing decreased viability and altered morphology of CKO cells.

(D) Quantification of viability of control and CKO cells at 1 to 4 days differentiation.

(E) Affymetrix expression levels of selected OPC markers NG2, PDGFRα, and Ki67 for control and CKO cells at 4 days differentiation; CKO cells display normal downregulation of these markers.

(F) Expression levels of selected oligodendrocyte lineage markers in CKO cells at 4 days differentiation relative to control cells.

(G) Venn diagram showing overlap of genes induced >4-fold with OL differentiation and those repressed >4-fold in CKO relative to control cells.

(H) Schematic of transcriptional control of OL lineage specification and differentiation. MRF is required for the maturation of premyelinating OLs into mature OLs expressing the full complement of myelin genes, with its induction possibly regulated by YY1.

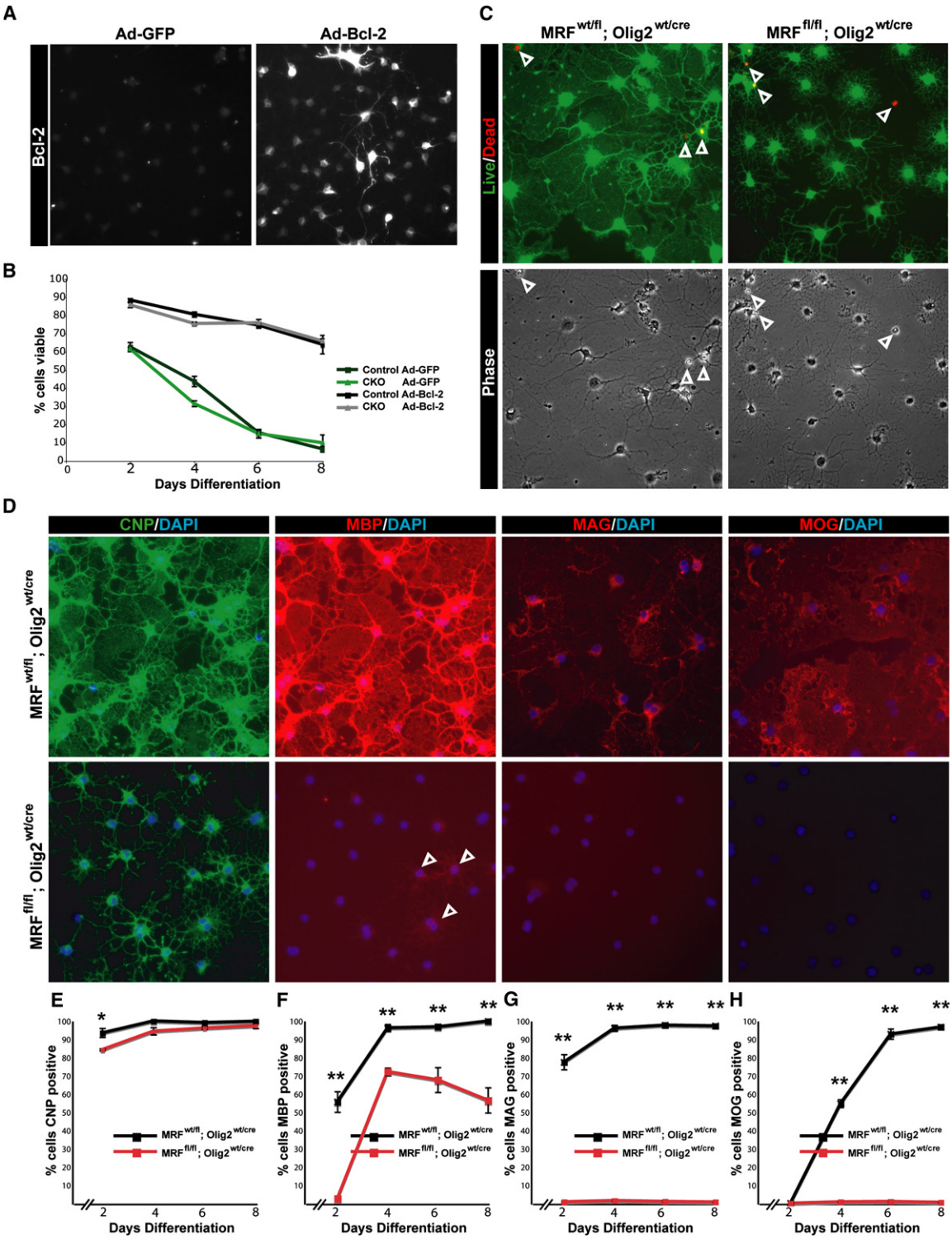

Figure 7. Blocking Apoptosis Does Not Restore Myelin Gene Expression in *MRF* CKO Oligodendrocytes

(A) Confirmation of Bcl-2 overexpression in Ad-BCL-2-infected cells.

(B) Viability of control and CKO cells infected with Ad-GFP or Ad-Bcl-2 over 8 days in differentiation media.

(C) Calcien-AM/ethidium homodimer and phase images of Ad-Bcl-2-infected control and CKO cells at 6 days differentiation showing viability and morphology. Arrowheads indicate dead cells.

(D) Expression of CNP, MBP, MAG, and MOG in Ad-Bcl-2-infected control and CKO cells at 6 days differentiation. Arrowheads indicate faintly MBP^{+} CKO cells.

(E–H) Quantification of the proportion of Ad-Bcl-2-infected control and CKO cells positive for CNP, MBP, MAG, and MOG at 2–8 days differentiation. $^{*}p < 0.05$, $^{**}p < 0.01$.

astrocytes and is upregulated strongly upon OL differentiation. In the absence of MRF, OPCs are able to withdraw from the cell cycle and differentiate into premyelinating OLs but are unable to mature, express the full complement of myelin genes, or myelinate and instead undergo apoptosis.

Montano et al. (2002) suggest that the yeast transcriptional activator Ndt80 may be the defining member of a family of transcription factors sharing a conserved DNA binding domain that includes *MRF/GM98* and *C11Orf9*. Here, we confirm a role for MRF in myelin gene regulation in OLs, and thus CNS myelination. The high degree of homology between MRF and C11Orf9, in addition to the ability of MRF to induce MBP expression in the chick, suggests that its function is likely to be conserved between mammalian and avian homologs. C11Orf9 mRNA is downregulated in fetal motor neuron/oligodendroglial dysfunction in humans (Pakkasjarvi et al., 2005), indicating that it may be expressed in OLs.

MRF's role is distinct from that of other transcription factors previously implicated in the OL lineage. MRF expression is restricted to postmitotic OLs and is required for expression of the vast majority of CNS myelin genes but not for OL specification or differentiation per se. Several OL lineage transcription regulators such as Nxk2.2, Olig1/2, Sox10, and YY1 are all expressed by OPCs as well as OLs, or in other CNS cell types (e.g., YY1). Although both *MRF* CKO and *Olig1*$^{-/-}$ mice have similar phenotypes with severe dysmyelination and death in the third week postnatal, it is not clear whether OLs differentiate in the *Olig1*$^{-/-}$ mice (Xin et al., 2005). Similarly, analysis of the spinal cords in *Sox10*$^{-/-}$ embryos suggests a role for Sox10 in promoting OL differentiation (Stolt et al., 2002). In contrast, *MRF* CKOs contain substantial numbers of premyelinating OLs at earlier ages but few myelinating OLs. Although Olig1 and Sox10 can activate specific myelin genes (Li et al., 2007; Stolt et al., 2002), Olig1 is not localized to the nucleus of myelinating oligodendrocytes (Arnett et al., 2004), suggesting that it may not directly induce myelin genes. So far, Nkx6.2 is the only transcription factor shown to be specific to postmitotic OLs. However *Nkx6.2*$^{-/-}$ mice show surprisingly few myelin deficits, with aberrations largely confined to the paranodal region (Southwood et al., 2004), which contrasts with those seen in *MRF* CKOs. Whereas the majority of transcription factors within the OL lineage are critical for the specification of OPCs or initial differentiation of OLs, MRF is unique in coordinating subsequent maturation/myelination of postmitotic OLs.

The role of MRF in the CNS appears analogous to the role of Krox-20 in the PNS. Krox-20 is expressed by myelinating Schwann cells and is both sufficient and necessary to drive the transition of a nonmyelinating Schwann cell to a myelinating state (Nagarajan et al., 2001; Topilko et al., 1994), and activate myelin gene promoters (Jang et al., 2006). As such, Krox-20 has been ascribed the role of a "master regulator" of PNS myelination. However, Krox-20 is not expressed within the CNS. The specificity of MRF expression to postmitotic OLs, both in the newly formed and more mature stages, in combination with the loss of myelin gene expression seen upon disruption of MRF function, suggests that MRF may have a functionally equivalent role to Krox-20 within the CNS. Interestingly, it is possible that MRF and Krox-20 share a common molecular switch that induces expression of both genes at the onset of myelination. Krox-20 expression is induced by the transcriptional regulator YY1 (He and Casaccia-Bonnefil, 2008). The *MRF* gene contains a YY1 consensus site within a highly conserved region in intron 1. Because YY1 has been shown to link the exit of OPCs from the cell cycle with their differentiation (He et al., 2007), the induction of MRF by YY1 or similar factors upon OPC differentiation may be a mechanism by which cell cycle exit is linked with OL differentiation and myelin gene expression.

How Does MRF Induce Myelination?

How does MRF induce myelin gene expression and myelination? Given its nuclear localization and conservation of the DNA binding domain with the yeast transcriptional activator Ndt80, MRF may function as a transcription factor in OLs. Consistent with this role, overexpression of a truncated form of MRF protein lacking the DNA binding domain in cultured OPCs failed to induce MBP expression (data not shown). Whether MRF functions as a bona fide transcriptional activator is an important question for future studies.

Although MRF is specific to OLs within the CNS, it is also expressed in other tissues such as lung and pancreas. Embryos lacking MRF in all tissues from germline deletion of MRF via a ubiquitous Cre driver failed to survive past ~E12.5 (data not shown). This indicates that MRF has additional roles unrelated to myelin gene expression outside the CNS. As such, MRF may cooperate with other factors to specifically induce myelin gene expression in OLs. Our observation that MRF overexpression in OPCs induced MBP and MOG in the majority of cells, whereas it induced only a small number of MBP^{+} cells in the spinal cord, strongly suggests that MRF may require other factors (e.g., Sox10) to drive myelin gene expression. Conversely, the confinement of MRF expression to the postmitotic phase of the OL lineage may explain why Sox10 (present at all stages of the OL lineage) can induce myelin gene expression only in postmitotic cells. MRF may control the expression of myelin genes directly by binding to their promoters, or alternatively it may indirectly induce the transition to a myelinating state by gating the expression of other transcription factors. Finally, in addition to myelin genes, MRF is required for the expression of a subset of other genes normally associated with OL maturation including Adamts4 and TPPP, a tubulin polymerase. It is therefore possible that MRF induces a cohort of genes during OL maturation that work together to assemble and wrap CNS myelin sheathes. Further analysis of MRF function and *MRF*-deficient mice will provide insights into these processes of CNS myelination independent of OL differentiation.

EXPERIMENTAL PROCEDURES

All animal procedures were approved by Stanford University's Administrative Panel on Laboratory Animal Care.

Isolation and Culture of Mouse OPCs

Detailed protocols for the purification and culture of mouse OL lineage cells are available upon request. Mouse OPCs were isolated from enzymatically dissociated P7 mouse brains as described (Cahoy et al., 2008), positively immunopanned for PDGFRα after a depletion of microglia with BSL1. Cells were

grown in serum-free media as previously described (Dugas et al., 2006), but with the addition of 2% B-27 (Invitrogen). PDGF-AA (10 ng/ml, PeproTech) was added to the media to proliferate OPCs; PDGF-AA was removed and triiodothyronine (T3) (40 ng/ml; Sigma) added to the media to induce differentiation.

Transfections of OPCs

Cultures of mouse OPCs were passaged and resuspended to 50 × 10^6 cells/ml in OPC Nucleofection solution (Amaxa). 100 μl (5 × 10^6 cells) was added to expression plasmids (~4 μg/transfection) or siRNAs (10 μl of 20 μM of siRNAs against MRF or siControl nontargeting siRNA pool) and electroporated with the Amaxa nucleofection apparatus. See Supplemental Experimental Procedures for more details.

Adenoviral Infection of OPCs

1 million OPCs of each genotype were cultured in proliferative conditions for 4 hr in the presence of Ad-Bcl2 or Ad-GFP (Vector Biolabs) at an MOI of 100 in 10 ml of media. After 4 hr, the media was changed and cells were passaged into differentiative conditions. Efficiency of infection was analyzed at 2 days after infection via GFP expression; infection efficiencies of >95% were obtained.

In Ovo Electroporations of Chick Embryos

Approximately 1 μl of DNA solutions (~4 μg/μl of a 1:4 mix of pCIG and pCAGGS-MRF and pCAGGS-Sox10 constructs) in TE buffer with 0.2% fast green to permit visualization were injected into the neural tube of HH stage 12 embryos. Electroporation was performed as described (Zhou et al., 2001). Embryos were harvested 4 days after electroporation and processed for in situ hybridization or immunohistochemistry.

Immunohistochemistry

10 μm tissue cryosections or cells grown on PDL-coated coverslips were fixed for 10 min in 4% paraformaldehyde in PBS for 10 min, washed in PBS, and then incubated for 30 min in blocking solution (10% FCS in PBS for surface antigens, with 0.3% triton-X for intracellular antigens). See Supplemental Experimental Procedures for list of antibodies used. Coverslips or slides were washed in PBS and incubated with the appropriate fluorophore-conjugated secondary (Molecular Probes, 1:500 in blocking solution), washed in PBS, and mounted in DAKO mounting medium with DAPI. Fluoromyelin (Invitrogen) staining was performed on 10 μm cryosections according to manufacturer's instructions.

In Situ Hybridization

An in situ hybridization probe corresponding to 941 bp from the MRF 3′ UTR was amplified from OL cDNA with the primers GGTGGGTTTGAGTTTGGA GGTT and GGGGAAACGCTCTATGAACAGG and subcloned into the PCR-II-Topo vector (Invitrogen). The PLP probe was a kind gift of William Richardson. In situ hybridizations were performed as described (Cahoy et al., 2008).

TEM Microscopy

Anesthetized P13 mice were perfused with PBS followed by 2% gluteraldehyde/4% paraformaldehyde in sodium cacodylate buffer. Optic nerves were dissected out and postfixed overnight at 4°C. After treatment with 1% osmium tetroxide and 1% uranyl acetate, nerves were embedded in epon. Sectioning and electron microscopy was performed at Stanford Microbiology and Immunology Electron Microscopy Facility. Blind counts of myelinated axons were performed on images of randomly selected areas of the optic nerves. At least 100 axons of 0.3 μm or greater diameter were counted from 5 images per animal.

Northern Hybridization

Total RNA (5–15 μg) was run on a denaturing gel, transferred to Hybond-N+ (Amersham), and UV crosslinked. Membranes were prehybridized for 2 hr in 100 ml hybridization solution (7% SDS, 0.5 M Na_2HPO_4 [pH 7.2], 100 μg/ml herring sperm DNA) at 68°C. Radioactively labeled DNA probes were generated from plasmids containing approximately 1 kb of MRF, CNP, PLP, or GAPDH cDNA with the Prime It II random Primer kit (Stratagene) as per manufacturer's instructions with [α-^{32}P]dCTP (GE Healthcare). Hybridization was allowed to occur at 68°C overnight, washed 2× 10 min in 1×SSC, 0.1% SDS at RT then 3× 10 min in 0.5×SSC, 0.1% SDS at 68°C. X-ray films (Amersham) were then exposed to the membrane at −80°C before being developed.

Affymetrix Analysis

Total RNA was isolated from cells with the RNeasy micro kit (QIAGEN, Valencia, CA) with QIAGEN on-column DNase treatment to remove any contaminating genomic DNA. The integrity of RNA was assessed with an Agilent 2100 Bioanalyzer (Agilent Technologies) and RNA concentration was determined with a NanoDrop ND-1000 spectrophotometer (NanoDrop, Rockland, DE). 1 μg total RNA was used for Affymetrix two-cycle target labeling and 430 2.0 Array hybridization according to manufacturer's instructions, see Supplemental Experimental Procedures for further details.

RT-PCR

RNA prepared as per above was subject to reverse transcription with Invitrogen Superscript III reverse transcriptase as per manufacturer's instructions. cDNA was subject to amplification for 25 or 30 cycles with gene-specific primers and run on 2% agarose gels.

Generation of *MRF* CKO Mice

Mice in which exon 8 of *MRF* was flanked by loxP sites were generated my cloning exon 8 into the Sal1 site of the pEZ-Frt-lox-DT targeting vector. A 5 kb 5′ arm and 3 kb 3′ arm were cloned into the Not1 and Xho1 sites, respectively, to enable targeting of homologous recombination into E14 ES cell line. Correctly targeted neomycin-resistant clones were identified by Southern blotting of HindIII-digested DNA and PCR verification of the insertion of the 5′ loxP site. Targeted cells were injected into blastocytes to generate chimeric mice. $MRF^{wt/fl}$ mice were crossed onto the FlpER strain (Farley et al., 2000) to delete the neomycin cassette. Heterozygous *MRF* floxed mice were crossed for two generations onto *Olig2-Cre* mice (Schuller et al., 2008) or *CNP-Cre* mice (Lappe-Siefke et al., 2003) to obtain $MRF^{fl/fl}$; $Olig2^{wt/cre}$ or $MRF^{fl/fl}$; $CNP^{wt/cre}$ mice. See Supplemental Experimental Procedures for genotyping primers.

Quantification and Statistics

Blind counts of cultured cells were performed on at least 3 coverslips per condition, with 10 fields of vision (20× objective) counted per coverslip. For quantification of tissue sections, 4–6 mice were used per genotype. Three sections were analyzed per mouse, with sections 60–100 μm apart photographed (×20 objective) for analysis (areas of counted regions were quantified in ImageJ). For quantification of activated Caspase 3+ cells, the number of immunopositive cells was quantified for 3 longitudinal optic nerve sections 60 μm apart per mouse at ×20 objective, the nerves were then photographed at low power (×4 objective), and areas of the nerves determined in ImageJ. Averages were calculated for each coverslip or mouse, and these results used to calculate means and SEMs for each experimental condition or genotype. Groups were compared with unpaired 2-way t tests and Bonferroni's correction for multiple comparisons.

ACCESSION NUMBERS

Array data have been deposited NCBI's GEO database (accession number GSE15303).

SUPPLEMENTAL DATA

Supplemental Data include Supplemental Experimental Procedures, nine figures, two tables, and one movie and can be found with this article online at http://www.cell.com/cell/supplemental/S0092-8674(09)00456-5.

ACKNOWLEDGMENTS

We thank Professor Klaus-Armin Nave for kindly providing the CNP-Cre mouse line. We are indebted to Lydia-Marie Joubert for processing samples for TEM and Elizabeth Zou for processing samples for Affymetrix analysis. This work was funded by the National Eye Institute (RO1 EY10257, B.A.B.)

and the Myelin Repair Foundation. B.E. is supported by an Australian NHMRC CJ Martin award.

Received: July 30, 2008
Revised: February 2, 2009
Accepted: April 8, 2009
Published: July 9, 2009

REFERENCES

Arnett, H.A., Fancy, S.P., Alberta, J.A., Zhao, C., Plant, S.R., Kaing, S., Raine, C.S., Rowitch, D.H., Franklin, R.J., and Stiles, C.D. (2004). bHLH transcription factor Olig1 is required to repair demyelinated lesions in the CNS. Science *306*, 2111–2115.

Barres, B.A., Hart, I.K., Coles, H.S., Burne, J.F., Voyvodic, J.T., Richardson, W.D., and Raff, M.C. (1992). Cell death and control of cell survival in the oligodendrocyte lineage. Cell *70*, 31–46.

Cahoy, J.D., Emery, B., Kaushal, A., Foo, L.C., Zamanian, J.L., Christopherson, K.S., Xing, Y., Lubischer, J.L., Krieg, P.A., Krupenko, S.A., et al. (2008). A transcriptome database for astrocytes, neurons, and oligodendrocytes: a new resource for understanding brain development and function. J. Neurosci. *28*, 264–278.

Dugas, J.C., Tai, Y.C., Speed, T.P., Ngai, J., and Barres, B.A. (2006). Functional genomic analysis of oligodendrocyte differentiation. J. Neurosci. *26*, 10967–10983.

Farley, F.W., Soriano, P., Steffen, L.S., and Dymecki, S.M. (2000). Widespread recombinase expression using FLPeR (flipper) mice. Genesis *28*, 106–110.

Fu, H., Qi, Y., Tan, M., Cai, J., Takebayashi, H., Nakafuku, M., Richardson, W., and Qiu, M. (2002). Dual origin of spinal oligodendrocyte progenitors and evidence for the cooperative role of Olig2 and Nkx2.2 in the control of oligodendrocyte differentiation. Development *129*, 681–693.

He, Y., and Casaccia-Bonnefil, P. (2008). The Yin and Yang of YY1 in the nervous system. J. Neurochem. *106*, 1493–1502.

He, Y., Dupree, J., Wang, J., Sandoval, J., Li, J., Liu, H., Shi, Y., Nave, K.A., and Casaccia-Bonnefil, P. (2007). The transcription factor Yin Yang 1 is essential for oligodendrocyte progenitor differentiation. Neuron *55*, 217–230.

Jang, S.W., LeBlanc, S.E., Roopra, A., Wrabetz, L., and Svaren, J. (2006). In vivo detection of Egr2 binding to target genes during peripheral nerve myelination. J. Neurochem. *98*, 1678–1687.

Kuhlbrodt, K., Herbarth, B., Sock, E., Hermans-Borgmeyer, I., and Wegner, M. (1998). Sox10, a novel transcriptional modulator in glial cells. J. Neurosci. *18*, 237–250.

Lappe-Siefke, C., Goebbels, S., Gravel, M., Nicksch, E., Lee, J., Braun, P.E., Griffiths, I.R., and Nave, K.A. (2003). Disruption of Cnp1 uncouples oligodendroglial functions in axonal support and myelination. Nat. Genet. *33*, 366–374.

Li, H., Lu, Y., Smith, H.K., and Richardson, W.D. (2007). Olig1 and Sox10 interact synergistically to drive myelin basic protein transcription in oligodendrocytes. J. Neurosci. *27*, 14375–14382.

Lu, Q.R., Yuk, D., Alberta, J.A., Zhu, Z., Pawlitzky, I., Chan, J., McMahon, A.P., Stiles, C.D., and Rowitch, D.H. (2000). Sonic hedgehog-regulated oligodendrocyte lineage genes encoding bHLH proteins in the mammalian central nervous system. Neuron *25*, 317–329.

Lu, Q.R., Sun, T., Zhu, Z., Ma, N., Garcia, M., Stiles, C.D., and Rowitch, D.H. (2002). Common developmental requirement for Olig function indicates a motor neuron/oligodendrocyte connection. Cell *109*, 75–86.

Montano, S.P., Cote, M.L., Fingerman, I., Pierce, M., Vershon, A.K., and Georgiadis, M.M. (2002). Crystal structure of the DNA-binding domain from Ndt80, a transcriptional activator required for meiosis in yeast. Proc. Natl. Acad. Sci. USA *99*, 14041–14046.

Nagarajan, R., Svaren, J., Le, N., Araki, T., Watson, M., and Milbrandt, J. (2001). EGR2 mutations in inherited neuropathies dominant-negatively inhibit myelin gene expression. Neuron *30*, 355–368.

Pakkasjarvi, N., Gentile, M., Saharinen, J., Honkanen, J., Herva, R., Peltonen, L., and Kestila, M. (2005). Indicative oligodendrocyte dysfunction in spinal cords of human fetuses suffering from a lethal motoneuron disease. J. Neurobiol. *65*, 269–281.

Qi, Y., Cai, J., Wu, Y., Wu, R., Lee, J., Fu, H., Rao, M., Sussel, L., Rubenstein, J., and Qiu, M. (2001). Control of oligodendrocyte differentiation by the Nkx2.2 homeodomain transcription factor. Development *128*, 2723–2733.

Schuller, U., Heine, V.M., Mao, J., Kho, A.T., Dillon, A.K., Han, Y.G., Huillard, E., Sun, T., Ligon, A.H., Qian, Y., et al. (2008). Acquisition of granule neuron precursor identity is a critical determinant of progenitor cell competence to form Shh-induced medulloblastoma. Cancer Cell *14*, 123–134.

Southwood, C., He, C., Garbern, J., Kamholz, J., Arroyo, E., and Gow, A. (2004). CNS myelin paranodes require Nkx6–2 homeoprotein transcriptional activity for normal structure. J. Neurosci. *24*, 11215–11225.

Stohr, H., Marquardt, A., White, K., and Weber, B.H. (2000). cDNA cloning and genomic structure of a novel gene (C11orf9) localized to chromosome 11q12→q13.1 which encodes a highly conserved, potential membrane-associated protein. Cytogenet. Cell Genet. *88*, 211–216.

Stolt, C.C., Rehberg, S., Ader, M., Lommes, P., Riethmacher, D., Schachner, M., Bartsch, U., and Wegner, M. (2002). Terminal differentiation of myelin-forming oligodendrocytes depends on the transcription factor Sox10. Genes Dev. *16*, 165–170.

Topilko, P., Schneider-Maunoury, S., Levi, G., Baron-Van Evercooren, A., Chennoufi, A.B., Seitanidou, T., Babinet, C., and Charnay, P. (1994). Krox-20 controls myelination in the peripheral nervous system. Nature *371*, 796–799.

Trapp, B.D., Nishiyama, A., Cheng, D., and Macklin, W. (1997). Differentiation and death of premyelinating oligodendrocytes in developing rodent brain. J. Cell Biol. *137*, 459–468.

Xin, M., Yue, T., Ma, Z., Wu, F.F., Gow, A., and Lu, Q.R. (2005). Myelinogenesis and axonal recognition by oligodendrocytes in brain are uncoupled in Olig1-null mice. J. Neurosci. *25*, 1354–1365.

Zhou, Q., and Anderson, D.J. (2002). The bHLH transcription factors OLIG2 and OLIG1 couple neuronal and glial subtype specification. Cell *109*, 61–73.

Zhou, Q., Choi, G., and Anderson, D.J. (2001). The bHLH transcription factor Olig2 promotes oligodendrocyte differentiation in collaboration with Nkx2.2. Neuron *31*, 791–807.